technical transactions

No. 2026/002

mechanics

Paradigm

Analysis of parametric vibrations of a tensioned string using non-contact measurement methods

Andrzej Czerwiński

andrzej.czerwinski@pk.edu.pl | https://orcid.org/0000-0003-3245-6398

Cracow University of Technology,
Faculty of Mechanical Engineering

Scientific Editor: Grzegorz Filo,
Cracow University of Technology
Technical Editor: Dorota Sapek,
Cracow University of Technology Press
Typesetting: Anna Pawlik,
Cracow University of Technology Press

Received: May 30, 2025
Accepted: October 1, 2025

Copyright: © 2026 Czerwiński. This is an open access article distributed under the terms of the Creative Commons Attribution License, which permits unrestricted use, distribution, and reproduction in any medium, provided the original author and source are credited.

Data Availability Statement: All relevant data are within the paper and its Supporting Information files.

Competing interests: The authors have declared that no competing interests exist.

Citation: Czerwiński, A. (2026). Analysis of parametric vibrations of a tensioned string using non-contact measurement methods. *Technical Transactions, e2026002*. https://doi.org/10.37705/TechTrans/e2026002

Abstract

This paper presents the results of an experimental study of the parametric vibrations of a pulsating tensioned string. At certain amplitudes and frequencies of excitation in the form of a variable axial force, dynamic instability arises in the system, and transverse vibrations are excited. A non-contact measurement system based on high-speed cameras and an image analysis method was used for the measurements. The eigenfrequency values of the system were determined, and the different types of resonant vibrations arising were examined in detail. In each case, the mode shape of the vibrations, motion trajectories, time traces, spectra and phase portraits of the vibrations were studied. Vibrations in single-mode simple resonances with periodic type and in-plane motion, spatial non-periodic vibrations in combination resonances and also cases of very complex non-periodic vibrations with spatial motion when different types of parametric resonances excite simultaneously were identified.

Keywords: dynamic instability, parametric resonance, image analysis, 3D-motions

1. Introduction

Parametric vibrations of continuous systems such as strings, rods, beams or plates are a problem often encountered in engineering practice and a topic analysed in many research works. Their importance stems from the fact that they can often pose a threat to the stability or durability of structures. On the other hand, they are also a very interesting physical phenomenon in themselves, for the study of which many different theoretical as well as experimental methods are used. Parametric resonance is a dynamic instability of a system arising when a specific parameter of the system (e.g. stiffness, length) varies periodically. The highest probability of excitation of parametric oscillations occurs when the ratio of the forcing frequency and the eigenfrequency of the system assumes certain specified values (e.g. multiples). Characteristically, the vibration amplitude during resonant excitation increases approximately exponentially (in the unstable phase) and then, in real systems, due to their non-linearity, reaches a steady state (limit cycle oscillation). In continuous systems, parametric resonances are associated with specific modes of natural vibration. In the simplest case, when the parametric vibrations are associated with a single mode of vibration, a simple resonance is induced. It is most easily excited when the frequency of the parametric excitation is twice the frequency of the eigenmode (main resonance), but can also form when the frequency of the excitation is two, three, etc. times smaller (secondary resonances). When several eigenmodes (usually two) are excited simultaneously during a resonance, this is called a combination resonance. The excitation of this type of vibration occurs most easily when the excitation frequency is equal to the sum of the eigenfrequencies of the component modes of the resulting resonance.

Studies on parametric vibrations usually focus on investigating the stability conditions of systems (using linear models) or, using non-linear models, on analysing the nature of the induced vibrations. The effects on stability of many system parameters are studied, most often the frequency and amplitude of parametric excitation, support conditions, additional concentrated masses, system curvature, etc. The phenomenon of parametric vibrations is studied for axially moving systems (such as belts, tapes) where conditions for the excitation of resonances are created as a result of pulsations in the speed of motion (Ghayesh, 2012; Malookani, van Horssen, 2016; Sahoo, Panda, Pohit, 2016; Qing et al., 2024). In beam systems that are subjected to a cyclically varying compressive axial force, parametric resonances can arise (Sochacki, 2008; Huang et al., 2017; Farokhi, Ghayesh, 2018; Wang, Zhu, 2022). Similarly, the pulsating velocity of the fluid in the pipes produces a varying axial force that leads to the excitation of parametric oscillations (Semler, 1996; Panda, Kar, 2008; Li et al., 2018; Xie et al., 2020). Parametric vibrations have also been investigated in systems such as, e.g., beams subjected to variable transverse forcing (Huang et al., 2011; Zhai et al., 2022), cables used as e.g. supports for structures in which a variable force is generated by the movement of supports or the structure itself (Wei et al., 2016; Demšić et al., 2019) or more complex beam systems (e.g., frames) (Briseghella, Majorana, Pellegrino, 1998; Li, Shen, Que, 2024).

In experimental works, various measurement methods are used to study the movement of systems, which can generally be divided into contact and non--contact methods. If the mass and construction of the system under test allow it, it is possible to attach the sensor directly to the object under test. In this case, acceleration measurement using accelerometers attached at specific points in the structure (Ji, Hansen, 2000; Zhang et al., 2016; Liu et al., 2016; Czerwiński, Łuczko, 2021) or glued-on strain gauges (Lee, Poon, Ng, 2006) is the most common method. In many cases, e.g. due to the low stiffness or low mass of the system under test, contact measurements requiring the attachment of a sensor with additional mass are not feasible. In such cases, non-contact methods based on laser vibrometry (Kreider, Nayfeh, 1996; Nagai et al., 2007)

https://doi.org/10.37705/TechTrans/e2026002

or proximity sensors (Hwang, Perkins, 1994) that allow displacement measurements at selected points in the system can be used. Vision methods can also be used based on image registration using cameras and subsequent analysis (Zhang et al., 2004; Gonzalez-Buelga et al., 2008). With this method, simultaneous measurement of the movement of multiple points in the system can be performed and observation of, for example, vibration modes as a whole. Among the experimental studies mentioned above, the closest case to this study, was considered in Zhang et al. (2004). In that study, a vibrating frame suspended on two cables was examined. A simple parametric resonance was identified in the system as a result of harmonic excitation from the vibrating frame. Using image analysis from CCD cameras, the motion of the cables was observed and the damping coefficients were determined. An accelerometer on the suspended frame was used to determine the displacement and frequency during resonant vibrations. In the work (Gonzalez-Buelga et al., 2008), image analysis from high-speed cameras was used to investigate the natural frequencies and the stability limit in simple parametric resonance. The object under study was a diagonally suspended cable in which one of the supports performed a vertical harmonic motion. The other works mentioned above concern case studies such as forced vibrations of beams or vibrations of cables serving as suspension bridges.

This paper presents the results of the analysis of the parametric vibrations of a flexible solid silicone string subjected to a cyclically varying tensile axial force. Although the literature on parametric vibration of systems is very extensive, it contains mainly theoretical papers. Experimental articles are few in relation to these, and for the most part, these are papers published quite a long time ago. The changing techniques of measurement and data analysis nowadays allow a more detailed and comprehensive approach to experimental research. The studies presented in this paper using high-speed cameras include vibration analyses in selected ranges of simple and combination resonances, showing both the methodology of such studies and the interesting dynamic phenomena arising.

2. Research methodology

In order to perform tests on parametric vibrations, a test rig was built, the components and concepts of which are shown in Fig. 1. The rig consists of two functional parts: a system for forcing the vibrations of the test object and a system for measuring and recording the object's motion. The test object (silicone string) is placed vertically and fixed at both ends. The upper mount is stationary, and the lower mount is rigidly fixed to the vibration exciter head. An electromagnetic exciter of the Dongling Technologies ES-10-240 type was used here, with a maximum head displacement amplitude of 50 mm and a force of 10 kN. The string under test is statically tensioned in the axial direction by a constant force of 15 N. The exciter head, together with the lower clamp, performs movement in the vertical direction (along the axis of the tested object). This movement produces an additional time-varying axial force component. The amplitude and frequency of the pulsating force component are determined by the RULA RL-C21 type exciter controller, together with the VisProbe_SL software. To measure the value of the axial force in the system, a KMM20E-200N type transducer is mounted at the top handle, from which an analogue voltage signal is sent to the input of the A/D converter of the RULA RL-C21 controller.

Two high-speed cameras of the Kron Chronos 1.4 type were used to measure the vibration displacement of the tested object. They are fixed at half the length of the string at a distance of approx. 1.8 m from the test object. The cameras are located perpendicular to each other so that their field of observation covers the two mutually perpendicular planes in which the test

object is fixed. The operation of the cameras is synchronised in time, so that the position of the object at a given moment in time corresponds to the same frame number in both cameras. The cameras record sequences of approximately 4s at a speed of 3600 fps. Six markers are placed on the tested string at $L/7$ distances to facilitate motion analysis at specific points.

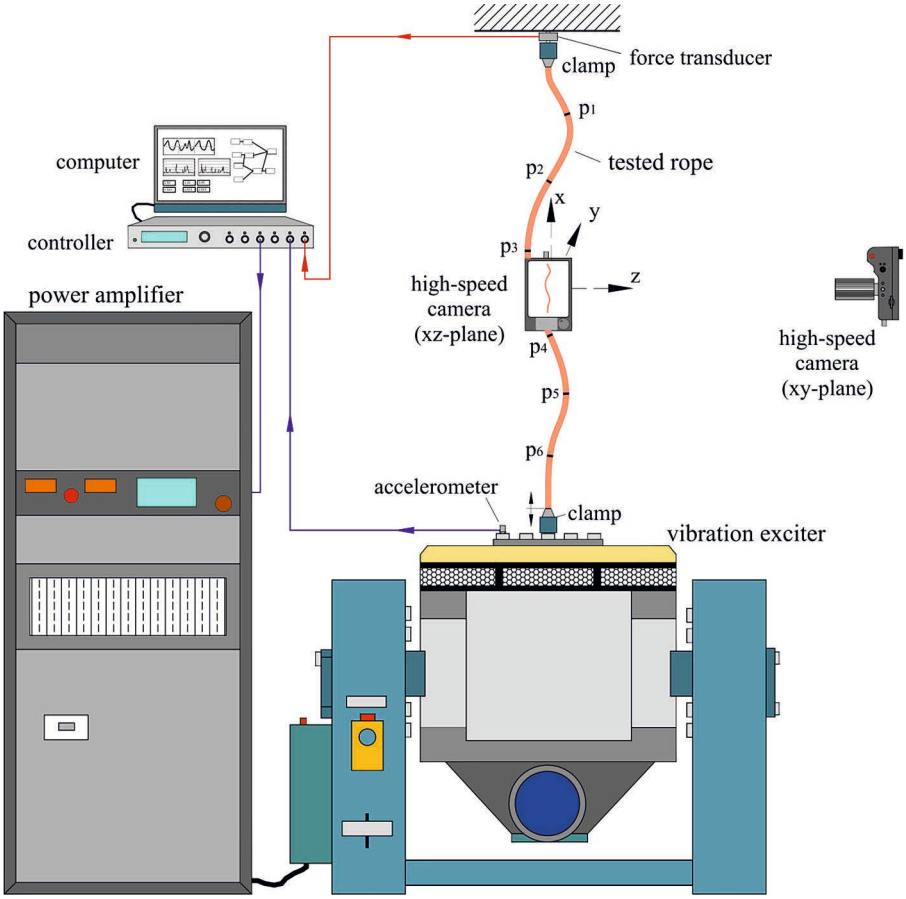

Fig. 1. Schematic of the test stand (source: own elaboration)

The movement analysis is performed offline on the basis of the recorded video in the Tracker software. In a first step, an image analysis of the stationary object (reference frame, Fig. 2(a)) is performed, separately for each plane to be analysed. The image calibration is established according to the actual dimensions of the observed object, and the coordinate system in the observation plane is adopted. The relevant video with the recorded object in motion is then loaded into the environment, thus prepared (Fig. 2(b)).

In the next step, the area of the image whose change of position in successive frames is to be identified by the software is selected and recorded in the form of coordinate values (x, y or x, z) as a function of time, in steps consistent with the FPS value. In the case studied, the areas encompassing the markers on the string were marked, and therefore, the movement of the system was identified at six equally distant points. (Fig. 2c). The identified displacement value data for each point and direction are then processed using DasyLab 2020 software according to the schematic shown in Fig. 3.

In the first stage, the data is filtered using a 1 Hz high-pass filter. This operation is intended to remove the constant component, i.e. the static marker position value, from the data and leave only the dynamic – variable component. The next operation is low-pass filtering (100 Hz). The signal obtained after marker tracking in the image is somewhat noisy due to random micro--errors generated during identification (this is visible in the example motion trajectory and time diagrams in Fig. 4 – bright blue lines). This is manifested

https://doi.org/10.37705/TechTrans/e2026002

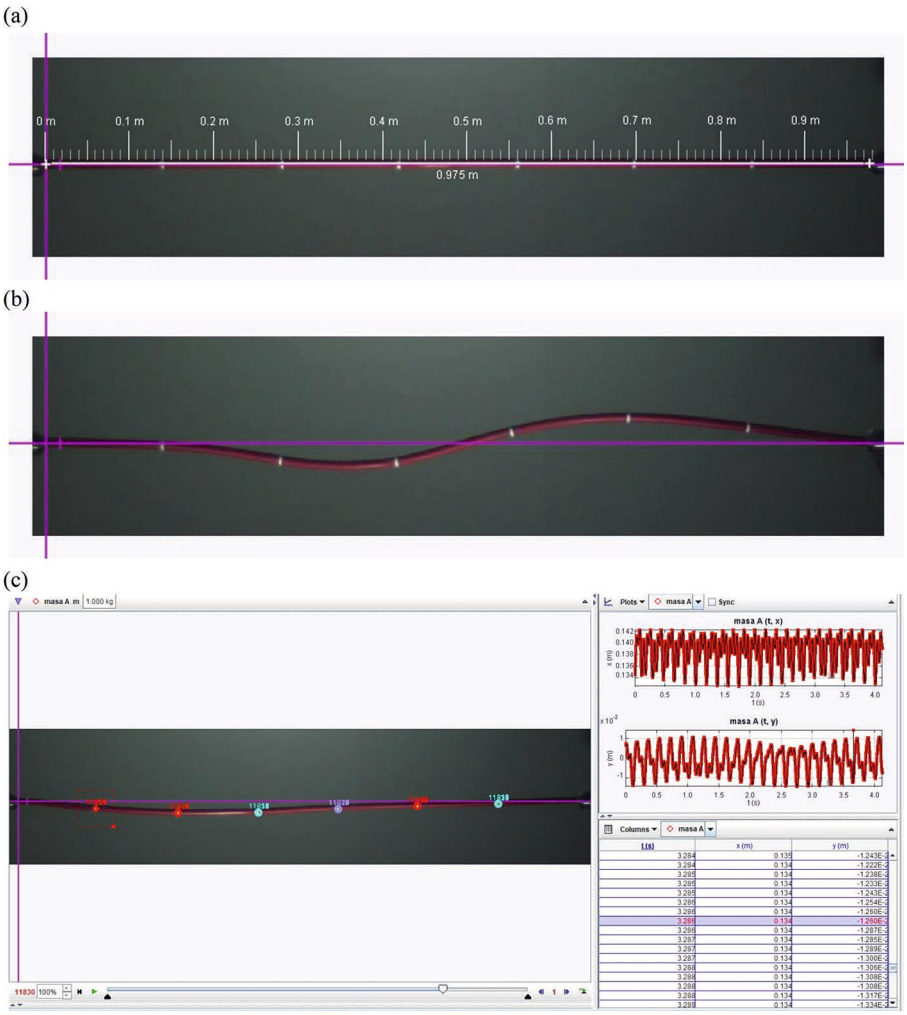

Fig. 2. Motion analysis in the Tracker software: (a) calibration of image dimensions on the reference frame, (b) frame with recorded system vibrations and marked markers, (c) identification of marker point movement (source: own elaboration)

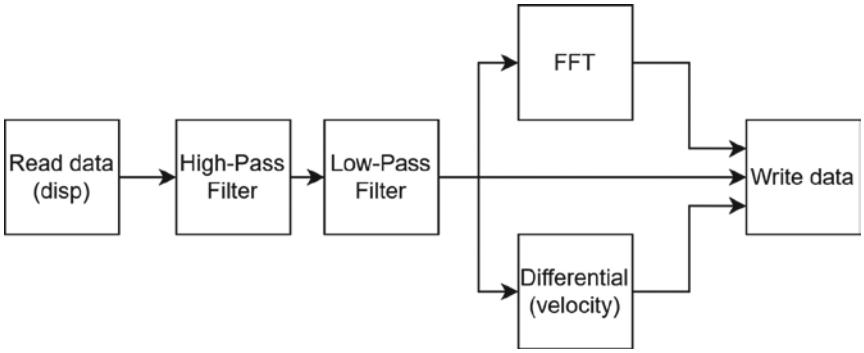

Fig. 3. Functional diagram of signal processing in DasyLab software (source: own elaboration)

by the presence of broadband noise in the signal spectrum, including at higher frequencies. However, since the frequency range of the vibration components of interest in the study is at most several dozen Hz, low-pass filtering significantly improves the quality of the measured signal (Fig. 4 – dark lines). The time histories additionally show delays introduced by the applied LP filters, but as the delays are the same for all signals (each vibration direction), they do not affect further analysis.

The signal processed in this way is then saved to a file and forms the basis for plotting or further analysis. A spectrum analysis of the signal using the FFT method with a resolution in the frequency domain of 0.25 Hz was used here. A conversion of the displacement signal into movement velocity using a numerical differentiation operation was also performed.

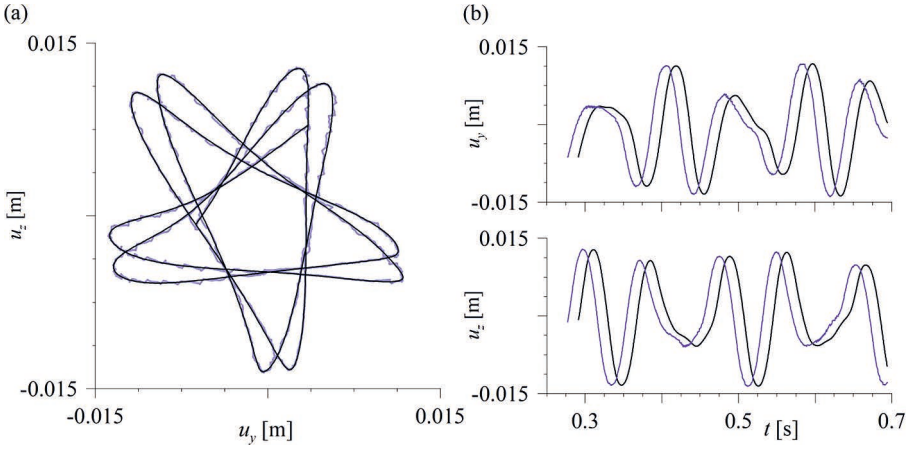

Fig. 4. Effect of low-pass filtering on vibration signals (a) motion trajectory, (b) time traces (light line – before filtering, dark line – after filtering) (source: own elaboration)

The signal processed in this way is then saved to a file and forms the basis for plotting or further analysis. A spectrum analysis of the signal using the FFT method with a resolution in the frequency domain of 0.25 Hz was used here. A conversion of the displacement signal into movement velocity using a numerical differentiation operation was also performed.

The string with a diameter of $d = 12$ mm and a circular cross-section with a length between fixing points of $L = 0.975$ m was chosen for the test. The material density was set at $\rho = 1220$ kg/m^3, and the measured Young's modulus has a value of $E = 7$ MPa. The string was subjected to an axial tensile force with a mean (static) value of $T_0 = 15$ N, varying according to the relationship $T = T_0(1 + a \sin 2\pi f_p t)$, where a is the amplitude of the force pulsation and f_p is the frequency of the force pulsation. For example, a value of parameter a equal to 0.2 means that the axial force pulsation is 20% of the static force T_0.

3. Test results

3.1. Free vibrations

Firstly, an analysis of the natural frequencies of the examined system was carried out.

Since the frequencies at which there is the greatest likelihood of exciting parametric resonances are closely related to the natural frequencies, knowing them greatly facilitates the search for the ranges in which parametric vibrations may be excited. The measurements were performed by briefly applying a force at the antinodes of successive vibration modes (e.g. for the first mode, in the centre of the system) and observing the decay of the oscillations. For each mode, vibrations were analysed at the point located closest to the antinode. Based on the recorded time traces, the natural frequencies of the first four φ modes and the logarithmic damping decrements Λ_i were determined. Fig. 5(a) shows the view of the second natural mode during the measurement (the image was created by combining successive frames from a video recording), while Fig. 5(b) presents the time traces of the first four modes. The displacement amplitudes in Fig. 5(b) were normalised by assuming a maximum value of 1 in each case.

From the analysis of the measured data, the frequencies and logarithmic decrements were determined: for the first mode $f_1 = 5.43$ Hz i $\Lambda_1 = 0.049$, for the second mode $f_2 = 11.11$ Hz i $\Lambda_2 = 0.060$, for the third mode $f_3 = 17.17$ Hz i $\Lambda_3 = 0.094$, for the fourth mode $f_4 = 23.90$ Hz i $\Lambda_4 = 0.132$.

https://doi.org/10.37705/TechTrans/e2026002

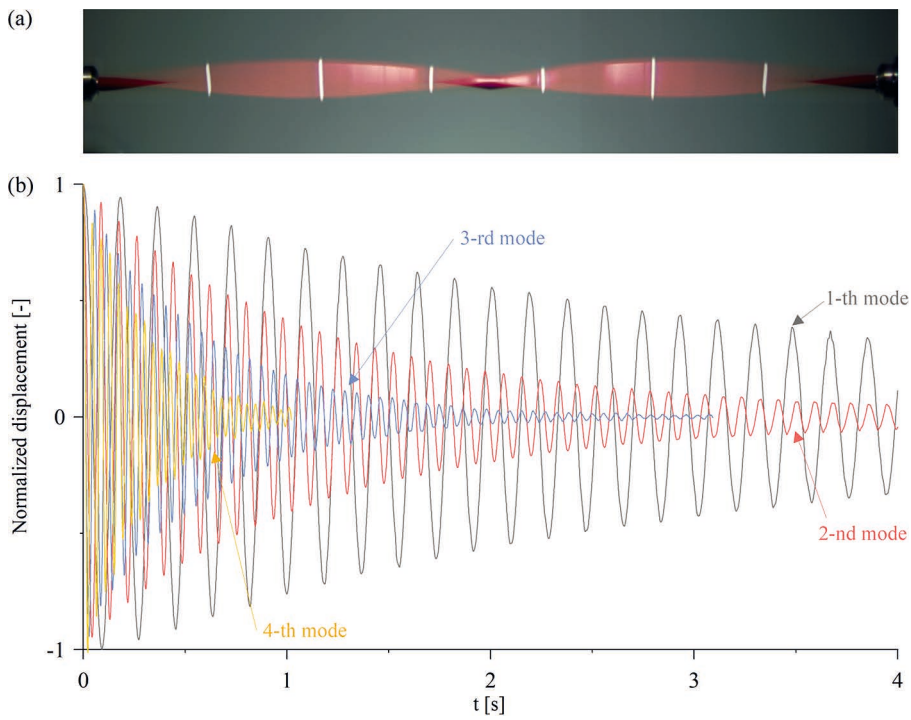

Fig. 5. Analysis of the natural vibrations of the system: (a) view of the second mode of free vibrations, (b) time traces of the free vibrations of four successive modes (source: own elaboration)

3.2. Parametric resonances

This section presents the results of investigations into the parametric vibrations of the system. During the test, the exciter generated a harmonic excitation with a specified frequency and amplitude. If certain conditions are met, transverse vibrations with a frequency different from that of the excitation are excited in the system. In the initial phase of instability, the vibration amplitude increases and, after a certain time, reaches a steady-state phase of vibration known as "limit cycle oscillations". The results presented in this section refer to observations of the system's vibrations, specifically in this steady-state phase of parametric resonance. Knowing the values of the eigenfrequencies makes it possible to preliminarily estimate at which excitation frequency (force pulsation) such vibrations may be induced. Single--mode principal parametric resonances occur when the excitation frequency is close to twice the eigenfrequency. Figs. 6 and 7 show the vibration analysis of the system for an excitation frequency of $f_p = 23.0$ Hz, which is approximately twice the natural frequency of the second mode $f_2 = 11.11$ Hz. The pulsation amplitude for the case studied is $a = 0.2$.

Fig. 6 shows in the centre a view of the modes of vibration in two planes $(x - y$ and $x - z)$, and above and below the trajectories of the system's motion in the transverse plane $(y - z)$ at selected points evenly spaced every $L/7$ distance. The views of the modes' shape were created by assembling about 1000 consecutive frames. As can be seen, the mode has one node in the centre and two antinodes at distances of approximately $L/4$ and $3L/4$, and this is the shape of the second eigenmode. From the observation of the motion trajectory, it can be seen that the vibration takes place in a plane oblique to the z and y directions. On the figures, at all points, this situation is represented by trajectory shapes in the form of line segments with the same inclination. The amplitudes of the vibrations vary from point to point and are obviously greatest near the antinodes (points p_2 and p_5). The modes' images show the motion trajectories of the six markers, and they have a dominant transverse component with some contribution from the axial component (line bending). This component comes from the forcing (movement of the end of the string) realised in the axial direction.

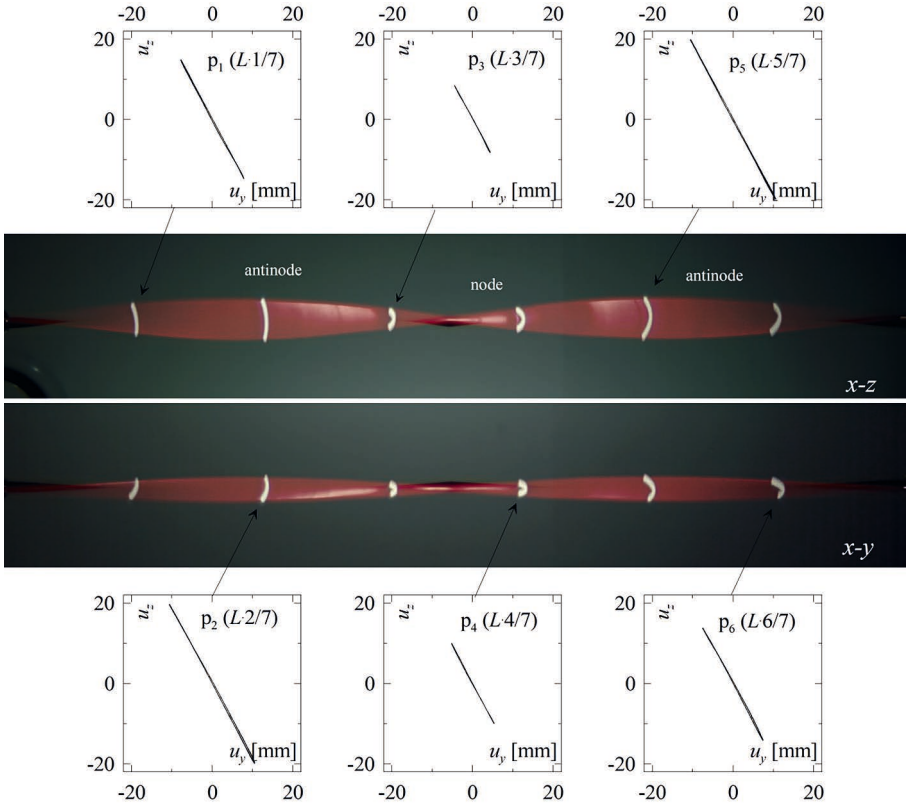

Fig. 6. Shape of vibration modes in the $x-z$ and $x-y$ planes and trajectories of motion in the transverse plane in the simple resonance of the second mode, for $f_p = 23.0$ Hz and $a = 0.2$ (source: own elaboration)

An analysis of the vibrations at p_2 $(2L/7)$ in the resonance case discussed here is shown in Fig. 7. The top three diagrams are for vibrations in the y--direction and the bottom three for vibrations in the z-direction. For each direction, time traces of the vibration displacement, spectrum, and a plot

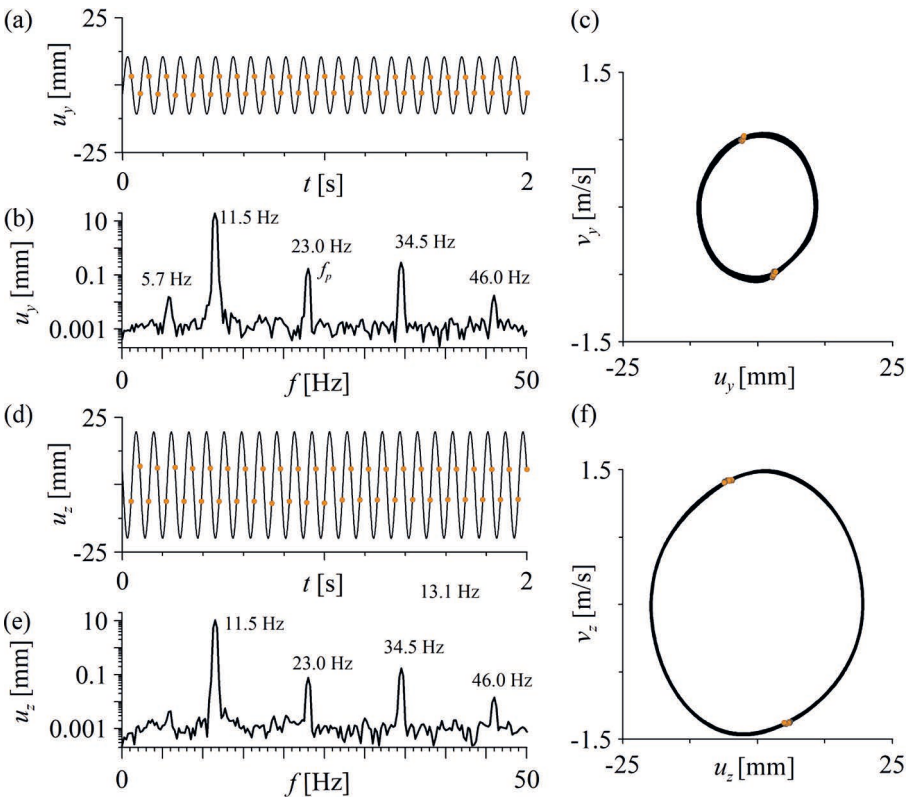

Fig. 7. Analysis of vibrations at p_2 for the case of simple resonance, ($f_p = 23.0$ Hz, $a = 0.2$): (a) time history in the y-direction, (b) spectrum in the y-direction, (c) phase portraits and Poincaré maps in the y-direction, (d) time history in the z-direction, (e) spectrum in the z-direction, (f) phase portraits and Poincaré maps in the z-direction (source: own elaboration)

https://doi.org/10.37705/TechTrans/e2026002

on the phase plane (displacement – velocity) with Poincaré map points are shown. The map was made using the stroboscopic method by recording successive points every one period of forcing (in the case under study, 1/23 Hz). Time traces show diagrams similar to periodic, harmonic oscillations. Here, there are two stroboscopic points per period, i.e. the oscillation has a frequency twice as low as the excitation frequency. This observation is confirmed by spectral analyses, where the clearly dominant component (11.5 Hz) is half the value of 23 Hz, i.e. the excitation frequency f_p. The value of 11.5 Hz is close to the eigenfrequency of the second mode (approx. 11.1 Hz), hence it is in this mode that the vibrations are excited. In addition to the main component, its third and fourth harmonics can be seen on the spectrum, as well as a component at the excitation frequency, but all these components have much smaller values. The diagrams on the phase plane have the shape of a closed curve similar to a circle and two points on a Poincaré map. Such a pattern is typical of periodic, sub-harmonic oscillations at twice the forcing frequency. The nature of the vibrations in the two directions analysed is the same, only quantitative differences can be noted due to the specific inclination of the vibration plane to the two directions.

Another type of parametric resonance arising in the studied system is shown in Fig. 8 and Fig. 9. This is an example of a combination resonance of two neighbouring modes (in this case, the second and third mode). The excitation frequency at which the analysed oscillations are induced is $f_p = 28$ Hz, and the amplitude of the axial force pulsation is $a = 0.275$. In contrast to the previously described case of simple resonance, the shape of the vibration mode in this case (Fig. 8) is not close to the shape of its eigenmode. There are no clear nodes and antinodes, only areas of smaller or larger amplitude. Three places of reduced amplitude can be observed here (in the middle and at about 1/3 and 2.3 of the length). The central decrease is related to the position of the node of the second mode included in the combination resonance, and the other two minima to the position of the nodes of the third mode. The amplitude maxima in the left and right parts of the system are, in turn, associated with the antinodes

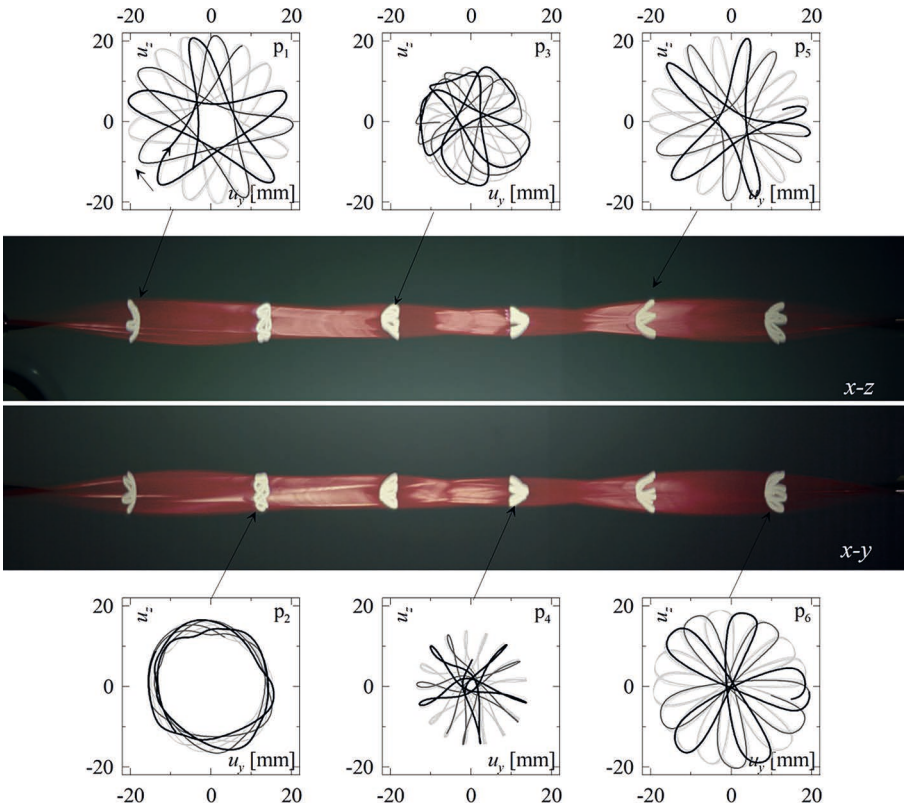

Fig. 8. Shape of vibration modes in the $x-z$ and $x-y$ planes and trajectories of motion in the transverse plane in the combination resonance of the second and third mode, for $f_p = 28.0$ Hz and $a = 0.275$ (source: own elaboration)

of both the second and third modes. Of interest are the trajectories of motion in the subfigures shown (Fig. 8), these are spatial vibrations with characteristic multi-vertex shapes. A distinct five vertices can be seen in each trajectory (bold dark line). As can be seen from (Czerwiński, Łuczko, 2018), such trajectories arise when the motion of the modes of the resonance components takes place in space, the modes spin around the system axis at different angular velocities and the resulting shape of the motion trajectory at a given point depends on the shape of the components' trajectories (usually ellipse-like figures), their amplitudes and frequencies. The frequency ratio of the resonance components determines the number of vertices of the resulting figures. In the case analysed, the components have frequencies of 11.5 Hz and 16.5 Hz (spectrum in Fig. 9), i.e. their ratio is about 1.43 and this is a number close to the fraction 3/2 and in such a case (Czerwiński, Łuczko, 2018) the resulting figure has five vertices (number of vertices = 2 + 3). However, because the frequency ratio is an irrational number, not exactly equal to 1.5, the figure of the motion trajectory performs a slow rotation (thinner, brighter lines on the subfigures, Fig. 8). At each of the analysed points, the shape of the trajectory is different, which is mainly due to different mutual proportions of the amplitudes of the resonance components at successive points. As can be seen from Fig. 9 and as mentioned above, two main components are excited in the resonance: those associated with the second mode, with a frequency of 11.5 Hz and those associated with the third mode, with a frequency of 16.5 Hz. The sum of these frequencies is equal to 28 Hz, which is the frequency of the excitation. This is a characteristic of the combination resonances. In addition to the main resonance components, other components with smaller amplitudes can be seen on the spectrum: a component with a pulsation frequency of 28 Hz and also components with frequencies that are the sum of the forcing frequency and the resonance components (39.5 Hz and 44.5 Hz). Time traces show non-periodic oscillations of a relatively time-ordered nature. This is confirmed by the pattern observed in the phase diagrams, which is characteristic of quasi-periodic oscillations (closed

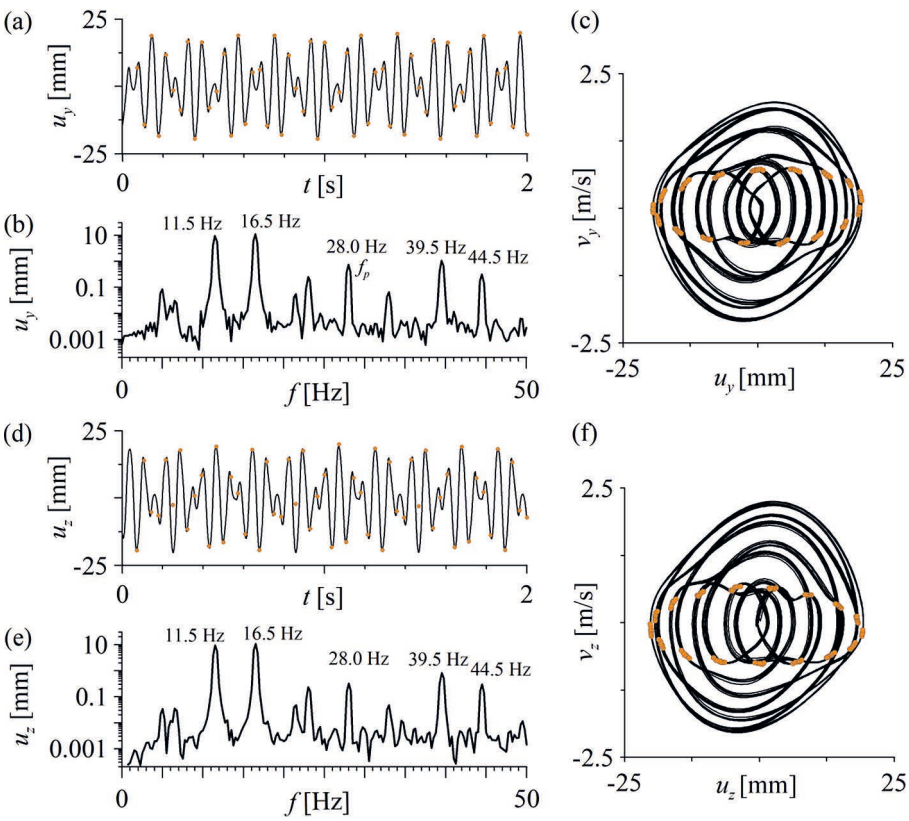

Fig. 9. Analysis of vibrations at p_1 for the case of combination resonance, ($f_p = 28.0$ Hz, $a = 0.275$): (a) time history in the y-direction, (b) spectrum in the y-direction, (c) phase portraits and Poincaré maps in the y-direction, (d) time history in the z-direction, (e) spectrum in the z-direction, (f) phase portraits and Poincaré maps in the z-direction (source: own elaboration)

https://doi.org/10.37705/TechTrans/e2026002

figure Poincaré map). The nature of the vibrations in the two analysed planes is quite similar both qualitatively and quantitatively.

The third example in the article (Fig. 10 and Fig. 11) concerns a vibration of an even more complex nature. The images of the vibration mode (Fig. 10) show a rather complex shape with many maxima and minima, not showing symmetry along the axis of the system and of a different nature and amplitude in each of the observed planes. Observation of the shapes of the motion trajectories at subsequent points confirms the above observation. The trajectories are complex, and it is difficult to find here the regularity observed in the previous case. The motion has a clear directionality diagonally with respect to y and z, but at the same time, it takes place in space along complicated lines. Some explanation of the nature of the analysed motion can be found in Fig. 11. The spectra show a dominant component with a frequency of 20 Hz, which is half of the forcing frequency (f_p = 40 Hz). This component is associated with the presence of a simple third-mode resonance. Since the motion in such resonances is flat, the trajectories (Fig. 10) show a clearly favoured direction of motion. In contrast, a combination resonance excited simultaneously with a simple resonance is responsible for the complex spatial motion. The spectrum shows clear components with frequencies of 14 Hz and 26 Hz, the sum of which is equal to the forcing frequency, and the frequency values can be correlated with the contribution of the second mode (14 Hz) and the fourth mode (26 Hz). In addition, the spectra show the contribution of many other components with frequencies resulting from the summation of the main component frequencies and pulsation frequencies, which further complicate the nature of the resulting vibrations. The time traces are non-periodic and disordered in nature, and the phase diagrams show diffuse point patterns (characteristic of vibrations of considerable complexity, including chaotic ones). It is interesting that the groups of scattered points are concentrated in two separated areas, which can be explained by the presence of a strong subharmonic periodic component of the simple resonance.

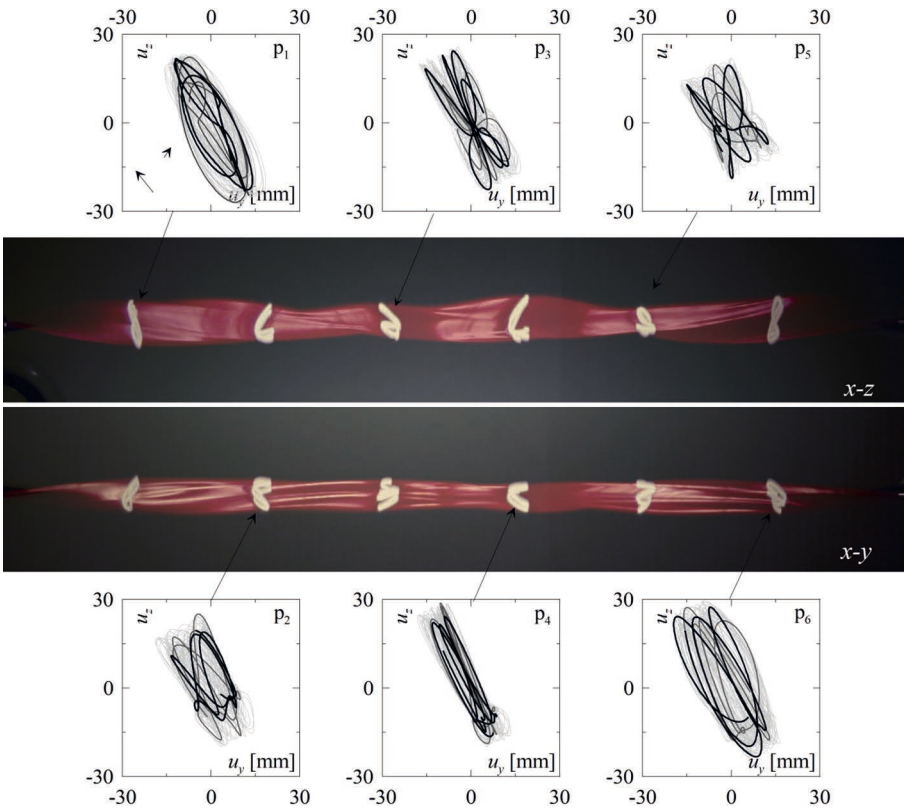

Fig. 10. Shape of vibration modes in the $x-z$ and $x-y$ planes and trajectories of motion in the transverse plane for the case of connected simple resonance of the third mode and combination resonance of the second and fourth modes, for $f_p = 40.0$ Hz and $a = 0.28$ (source: own elaboration)

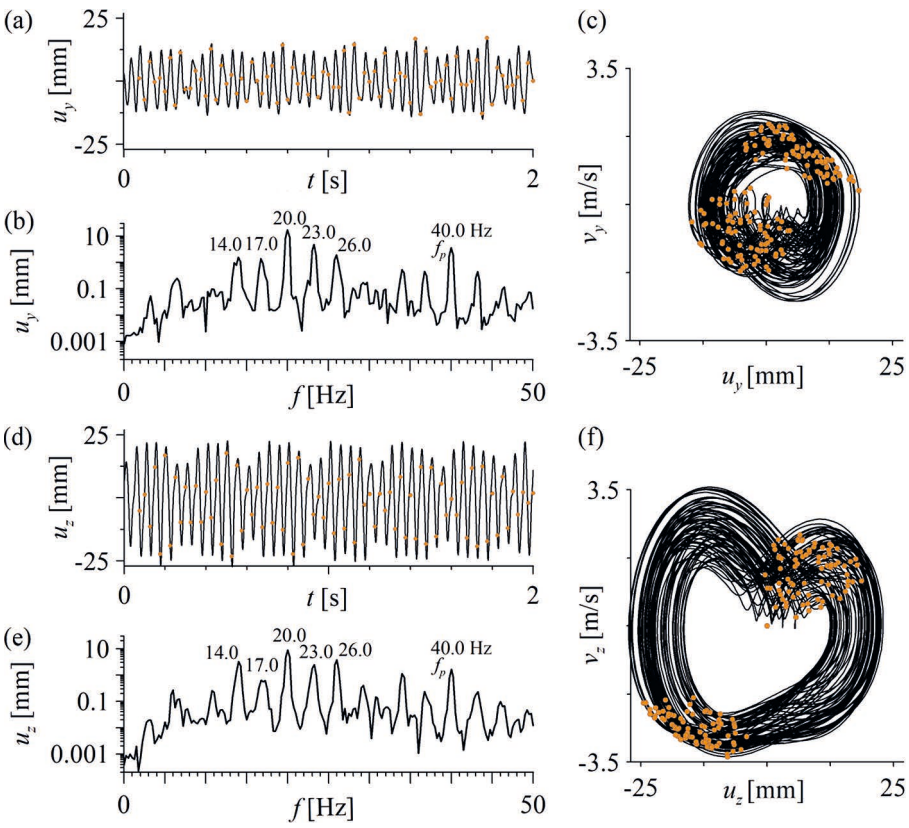

Fig. 11. Analysis of vibrations at p1 for the case of complex resonance, ($f_p = 40.0$ Hz, $a = 0.28$): (a) time history in the y-direction, (b) spectrum in the y-direction, (c) phase portraits and Poincaré maps in the y-direction, (d) time history in the z-direction, (e) spectrum in the z-direction, (f) phase portraits and Poincaré maps in the z-direction (source: own elaboration)

4. Conclusions

The article presents research on parametric vibrations of a string subjected to a pulsating axial force, conducted using a non-contact image analysis method. The methodology of the research is discussed in detail, and selected examples of the analysis of parametric vibrations excited in the system are shown. The possibility of exciting vibrations in resonances of various types was identified, such as: simple resonances of a single mode, combination resonances of two adjacent modes and complex resonances being a combination of different resonance types. In simple resonances, the vibrations take the shape of an eigenmode and occur in a plane. They arise when the excitation frequency is approximately twice the system's natural frequency and are periodic in nature. In combination resonances of adjacent modes, two components are excited, closely related to specific eigenmodes. The frequencies of these components are close to the natural frequencies of the respective modes, and their sum equals the excitation frequency. The excited vibrations are non-periodic – quasi--periodic, but relatively regular over time. Vibrations in this type of resonance have a spatial character, and the trajectories of motion in the transverse plane form characteristic multi-vertex figures. The shape and number of vertices in these figures depend on the relationship between the frequencies and amplitudes of the resonance components. If vibrations in multiple resonances are excited simultaneously in the system, they become significantly more complex. They are non-periodic and irregular over time, the vibration mode shape is complex, spatial, and variable, and the motion trajectories form intricate, irregular figures.

The measurement method applied in this study allows for determining the dynamic state of the system without influencing its parameters (as is the case with contact methods), which is a significant advantage, especially for flexible systems with low mass. The image analysis method enables the determination of motion parameters with sufficient precision and frequency,

https://doi.org/10.37705/TechTrans/e2026002

and simultaneously across the entire system under investigation. It is also an advantage that a direct measurement of the displacement is made here, the determination of which, for example, with accelerometers, involves double integration of the signal, which can, of course, result in the accumulation of calculation errors. Among the drawbacks of the method is the relatively high labour intensity associated with the analysis of the recorded image, as well as the inability to visualise results in real time.

Acknowledgments

The work was supported by funds from the Regional Operational Programme for the Małopolska Region for 2014–2020 entitled "Creation of Regional Group of Accredited Research and Calibration Laboratories of the Cracow University of Technology" No. RPMP.01.01.00-12-077/19-00-XVII/20/FE/20.

References

Briseghella, L., Majorana, C.E., Pellegrino, C. (1998). Dynamic stability of elastic structures: A finite element approach. *Computers & Structures*, 69, 11–25. https://doi.org/10.1016/S0045-7949(98)00084-4

Czerwiński, A., Łuczko, J. (2018). Non-planar vibrations of slightly curved pipes conveying fluid in simple and combination parametric resonances. *Journal of Sound and Vibration*, *413*, 270–290.

Czerwiński, A., Łuczko, J. (2021). Nonlinear vibrations of planar curved pipes conveying fluid, *Journal of Sound and Vibration*, *501*, 116054. https://doi.org/10.1016/j.jsv.2021.116054

Demšić, M., Uroš, M., Lazarević, A.J., Lazarević, D. (2019). Resonance regions due to interaction of forced and parametric vibration of a parabolic cable. *Journal of Sound and Vibration*, *447*, 78–104. https://doi.org/10.1016/j.jsv.2019.01.036

Farokhi, H., Ghayesh, M.H. (2018). Supercritical nonlinear parametric dynamics of Timoshenko microbeams. *Communications in Nonlinear Science and Numerical Simulation*, *59*, 592–605. https://doi.org/10.1016/j.cnsns.2017.11.033

Ghayesh, M.H. (2012). Subharmonic dynamics of an axially accelerating beam. *Archive of Applied Mechanics*, *82*(9), 1169–1181. https://doi.org/10.1007/s00419-012-0609-5

Gonzalez-Buelga, A., Neild, S.A., Wagg, D.J., Macdonald, J.H.G. (2008). Modal stability of inclined cables subjected to vertical support excitation. *Journal of Sound and Vibration*, *318*(3), 565–579. https://doi.org/10.1016/j.jsv.2008.04.031

Huang, J.L., Su, R.K.L., Lee, Y.Y., Chen, S.H. (2011). Nonlinear vibration of a curved beam under uniform base harmonic excitation with quadratic and cubic nonlinearities. *Journal of Sound and Vibration*, *330*(21), 5151––5164. https://doi.org/10.1016/j.jsv.2011.05.023

Huang, Y., Liu, A., Pi, Y., Lu, H., Gao, W. (2017). Assessment of lateral dynamic instability of columns under an arbitrary periodic axial load owing to parametric resonance. *Journal of Sound and Vibration*, *395*, 272–293. https://doi.org/10.1016/j.jsv.2017.02.031

Hwang, S.J., Perkins, N.C. (1994). High Speed Stability of Coupled Band/Wheel Systems: Theory and Experiment. *Journal of Sound and Vibration*, *169*(4), 459–483. https://doi.org/10.1006/jsvi.1994.1029

Ji, J.C., Hansen, C.H. (2000). Non-linear response of a post-buckled beam subjected to a harmonic axial excitation. *Journal of Sound and Vibration*, *237*(2), 303–318. https://doi.org/10.1006/jsvi.2000.3028

Lee, Y.Y., Poon, W.Y., Ng, C.F. (2006). Anti-symmetric mode vibration of a curved beam subject to autoparametric excitation. *Journal of Sound and Vibration*, *290*(1–2), 48–64. https://doi.org/10.1016/j.jsv.2005.03.009

Li, Q., Liu, W., Zhang, Z., Yue, Z. (2018). Parametric resonance of pipes with soft and hard segments conveying pulsating fluids. *International Journal of Structural Stability and Dynamics*, 18(10), 1850119. https://doi.org/10.1142/s0219455418501195

Li, Y., Shen, C., Que, Z. (2024). Vector form intrinsic finite element analysis for nonlinear parametric resonances of planar beam structures. *Journal of Sound and Vibration*, *584*, 118438. https://doi.org/10.1016/j.jsv.2024.118438

Liu, A., Lu, H., Fu, J., Pi, Y.L., Huang, Y., Li, J., Ma, Y. (2016). Analytical and experimental studies on out-of-plane dynamic instability of shallow circular arch based on parametric resonance. *Nonlinear Dynamics*, *87*(1), 677–694. https://doi.org/10.1007/s11071-016-3068-7

Kreider, W., Nayfeh, A. (1996). Experimental investigation of single-mode responses in a fixed-fixed buckled beam. In: *Dynamics Specialists Conference* (pp. 353–362). Salt Lake City, UT. https://doi.org/10.2514/6.1996-1247

Malookani, R.A., van Horssen, W.T. (2016). On Parametric Stability of a Nonconstant Axially Moving String Near Resonances. *Journal of Vibration and Acoustics*, *139*(1), 011005. https://doi.org/10.1115/1.4034628

Nagai, K., Maruyama, S., Sakaimoto, K., Yamaguchi, T. (2007). Experiments on chaotic vibrations of a post-buckledbeam with an axial elastic constraint. *Journal of Sound and Vibration*, *304*(3–5), 541–555. https://doi.org/10.1016/j.jsv.2007.03.034

Panda, L.N., Kar, R.C. (2008). Nonlinear dynamics of a pipe conveying pulsating fluid with combination, principal parametric and internal resonances. *Journal of Sound and Vibration*, *309*, 375–406. https://doi.org/10.1016/j.jsv.2007.05.023

Qing, J., Zhou, S., Wu, J., Shao, M., Tang, J. (2024). Parametric resonance of an axially accelerating viscoelastic membrane with a fractional model. *Communications in Nonlinear Science and Numerical Simulation*, *130*, 107691. https://doi.org/10.1016/j.cnsns.2023.107691

Semler, C. (1996). Nonlinear analysis of the parametric resonances of a planar fluid-conveying cantilevered pipe. *Journal of Fluids and Structures*, *10*(7), 787–825. https://doi.org/10.1006/jfls.1996.0053

Sahoo, B., Panda, L.N., Pohit, G. (2016). Combination, principal parametric and internal resonances of an accelerating beam under two frequency parametric excitation. *International Journal of Non-Linear Mechanics*, *78*, 35–44. https://doi.org/10.1016/j.ijnonlinmec.2015.09.017

Sochacki, W. (2008). The dynamic stability of a simply supported beam with additional discrete elements. *Journal of Sound and Vibration*, *314*(1–2), 180–193. https://doi.org/10.1016/j.jsv.2007.12.037

Wang, Y., Zhu, W. (2022). Supercritical nonlinear transverse vibration of a hyperelastic beam under harmonic axial loading. *Communications in Nonlinear Science and Numerical Simulation*, *112*, 106536. https://doi.org/10.1016/j.cnsns.2022.106536

Wei, M.H., Lin, K., Jin, L., Zou, D.J. (2016). Nonlinear dynamics of a cable--stayed beam driven by sub-harmonic and principal parametric resonance. *International Journal of Mechanical Sciences*, *110*, 78–93. https://doi.org/10.1016/j.ijmecsci.2016.03.007

Xie, W.D., Gao, X.F., Xu, W.H. (2020). Stability and nonlinear vibrations of a flexible pipe parametrically excited by an internal varying flow density. *Acta Mechanica Sinica*, *36*(1), 206–219. https://doi.org/10.1007/s10409-019-00910-w

Zhai, Y.J., Ma, Z.S., Ding, Q., Wang, X.P., Wang, T. (2022). Nonlinear transverse vibrations of a slightly curved beam with hinged–hinged boundaries subject to axial loads. *Archive of Applied Mechanics*, *92*(7), 2081–2094. https://doi.org/10.1007/s00419-022-02162-w

Zhang, L.N., Li, F.C., Yu, X., Cui, P.F., Wang, X.Y. (2016). Experimental Research on 2 : 1 Parametric Vibration of Stay Cable Model under Support Excitation. *Advances in Materials Science and Engineering*, 1–9. https://doi.org/10.1155/2016/9804159

Zhang, C.Y., Zhu, C.M., Lin, Z.Q., & Wu, T. X. (2004). Theoretical and Experimental Study on the Parametrically Excited Vibration of Mass--Loaded String. *Nonlinear Dynamics*, *37*(1), 1–18. https://doi.org/10.1023/b:nody.0000040034.86726.f5